Electronic Supplementary Material (ESI) for Physical Chemistry Chemical Physics.

Supplementary Information: Coronene: a model for ultrafast dynamics in graphene nanoflakes and PAHs

Alberto Martín Santa Daría,[1] Lola Gonzalez-Sanchez,[1] and Sandra Gómez[1,*]

[1] *Departamento de Química Física, Universidad de Salamanca, 37008 Salamanca, Spain*

* sandra.gomez@usal.es

I. BENCHMARKING

Benchmark calculations have been performed using different DFT functionals and basis sets to study the sensibility of the results with respect to the level of theory. The results showed here are supported by a previous benchmark study by B. Shi, *et al.*.[1]

In order to build stronger arguments when choosing the final level of theory, the absorption spectra has been computed using four different DFT functionals, namely B3LYP, PBE, wB97XD and CAM-B3LYP. Three different basis sets has been employed with these functionals: one double-zeta and one triple-zeta Pople basis sets, 6-31+G(d,p) and 6-311+G(d,p), including diffuse and polarized functions and one triple-zeta Dunning basis set, cc-pVTZ.

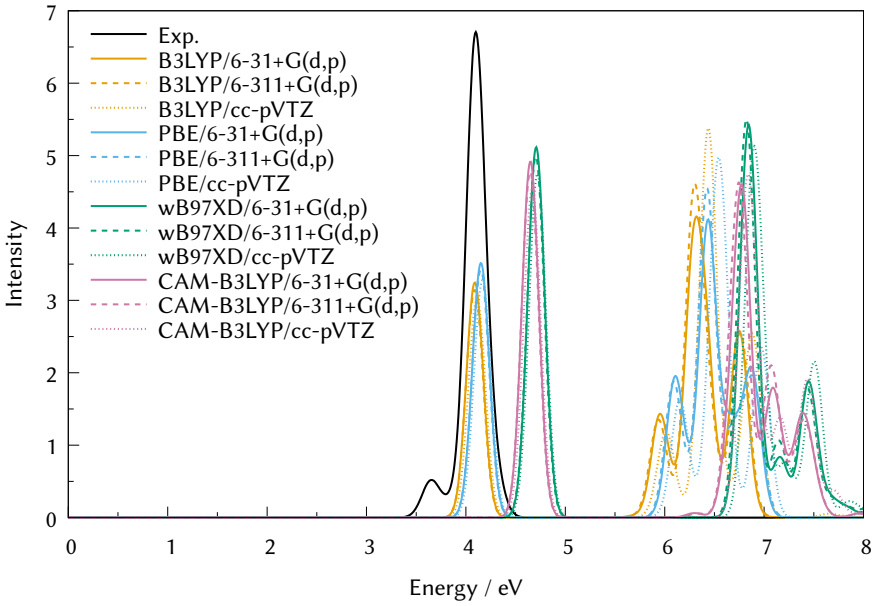

FIG. 1. UV/vis absorption spectrum of coronene. The experimental spectrum from Ref. 2, in black, is compared with the simulated spectra using different levels of theory.

The difference between the three basis sets performance is tiny, at least in the interesting region of the spectrum around the experimentally observed intense peak around 4 eV. Since the double-zeta basis 6-31+G(d,p) is the smallest and thus provides faster results, this has been selected as the final basis set to carry out the most expensive calculations.

Since we need to compute spin orbit couplings, we need to use ORCA 5.0 and its interface with SHARC. For this reason, instead of using 6-31+G(d,p) we use def2-SVP basis, implemented in ORCA and directly compared to 6-31+G(d,p) in bibliography.

Concerning the methods, and focusing again in the intense peak, it can be clearly observed in Fig. 1 that B3LYP and PBE reproduce better the experiments than CAM-B3LYP and wB97XD, thought these last two include, in principle, more corrections. The difference between B3LYP and CAM-B3LYP methods was analyzed by computing the vibrationally resolved absorption spectrum by computing the excitations from 10 initial structures generated using a Wigner distribution. The 3 different spectra are represented in Fig. 2, where it can be seen that the difference between the B3LYP and the CAM-B3LYP peaks is reduced when the vibrational correction is included using the Wigner distribution.

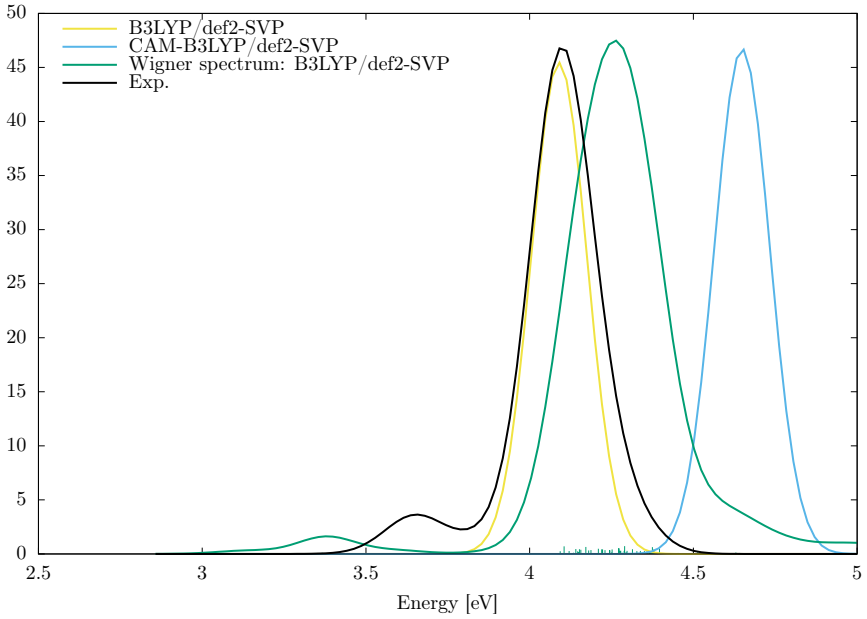

FIG. 2. Absorption spectrum of coronene comparing the experiments (black) with respect to B3LYP (yellow), CAM-B3LYP (blue) and the vibrationally resolved B3LYP (green) using 10 initial conditions from a Wigner distribution.

In order to study this ∼0.5 eV difference between the DFT methods, calculations have been carried out using the wave function method EOM-CCSD. The differences between the DFT methods and the EOM-CCSD has been represented in Fig. 3. Both CAM-B3LYP and wB97XD show better results when compared to the wave function method, while are further away from the experimental result than B3LYP and PBE.

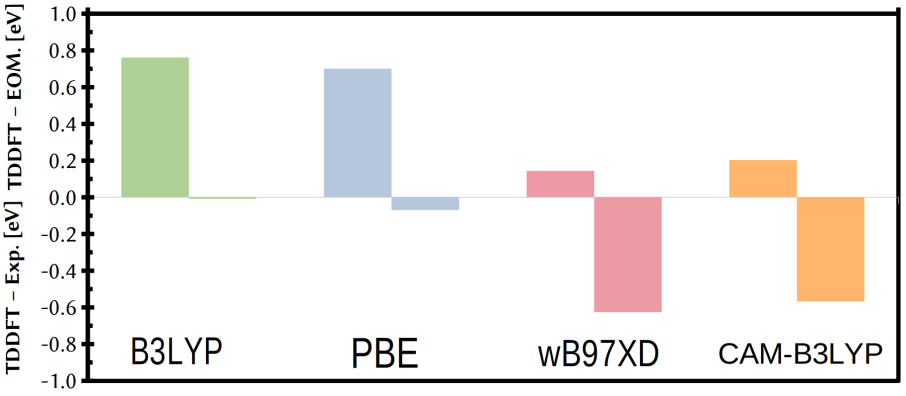

FIG. 3. Differences in the energy (in eV) of the brightest electronic state obtained using the four DFT functionales with respect to the experimental value (in negative values) and the EOM-CCSD (in positive values) using the 6-31+G(d,p) basis set.

From this benchmark study, it can be concluded that B3LYP/6-31+G(d,p) level of theory produces a good compromise between time consumption and numerical accuracy, at least when the results are going to be compared with respect to experimental observable. This can be explained by the error cancellation occurring when using this DFT functional.

II. NORMAL MODE ANALYSIS IN CORONENE

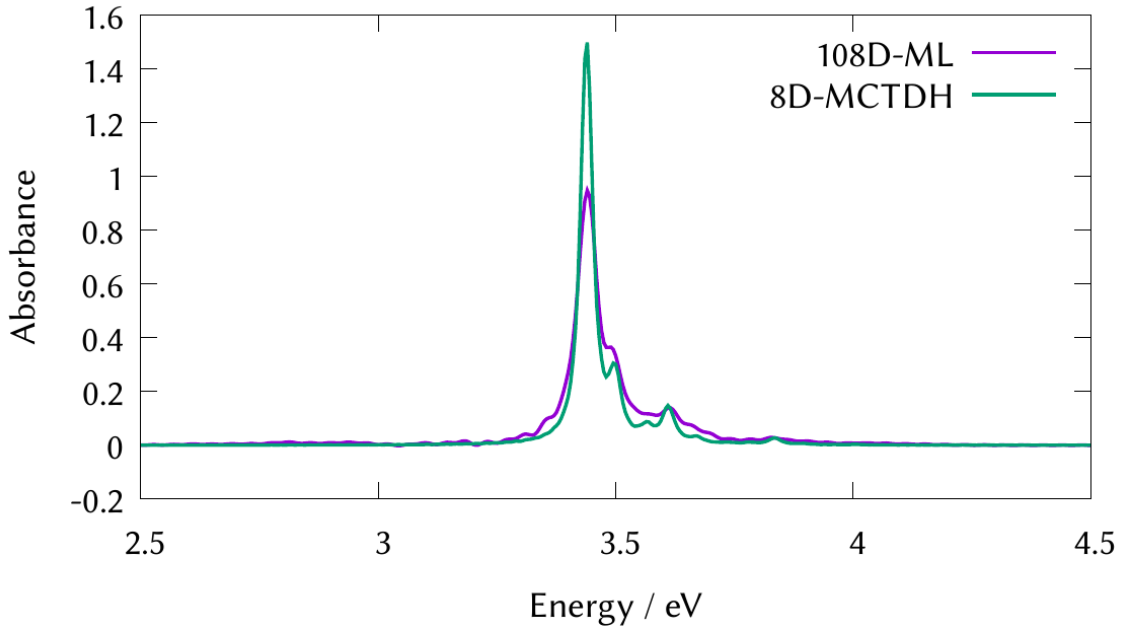

FIG. 4. Second band of the absorption spectrum of coronene obtained from the autocorrelation function of the quantum dynamics from $2B_{3u}$ (S_6) excited state after using the Fourier Transformation (FT). The purple line corresponds to the full calculation including the 108 normal modes and the green line includes only the 8 most relevant modes (ν_{24}, ν_{77}, ν_{60}, ν_{108}, ν_{19}, ν_{88}, ν_{64}, ν_{79})

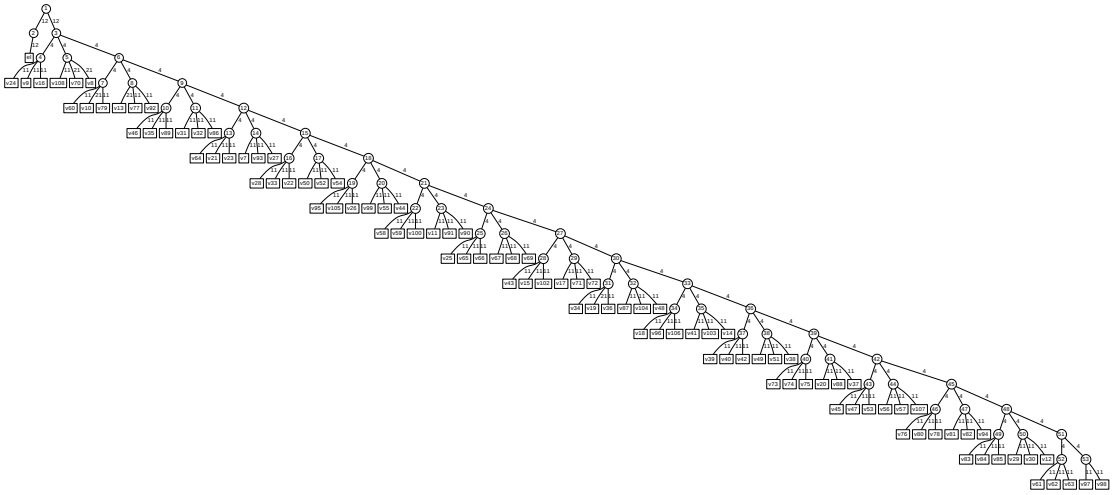

FIG. 5. Largest SPF basis used for the ML-MCTDH dynamics of coronene on the LVC potentials. The numbers on the last layer correspond to the number of primitive harmonic oscillator DVR functions used.

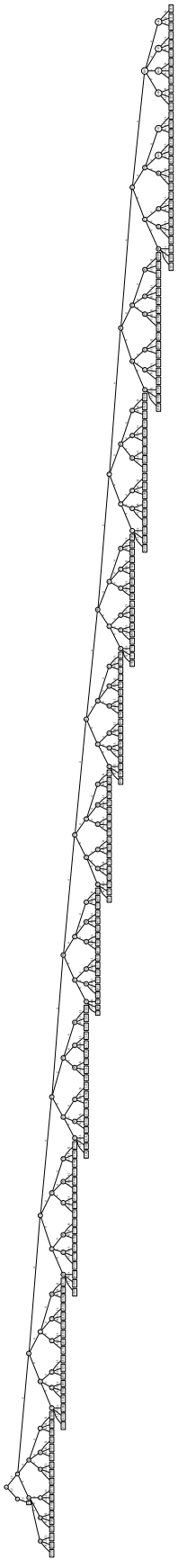

FIG. 6. Largest SPF basis used for the ML-MCTDH dynamics of circumcoronene on the LVC potentials. The numbers on the last layer correspond to the number of primitive harmonic oscillator DVR functions used.

III. EXCITED STATES QUANTUM DYNAMICS OF CORONENE

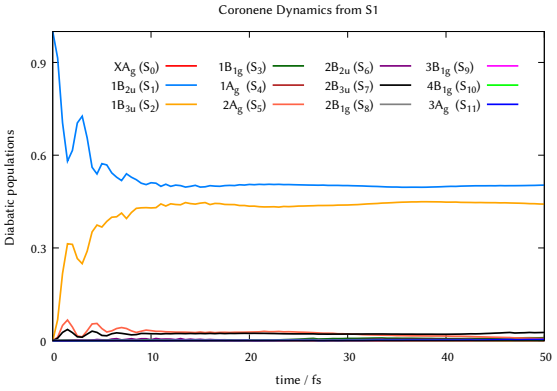

FIG. 7. Diabatic population transfer from $1B_{2u}(S_1)$ electronic excited state of coronene.

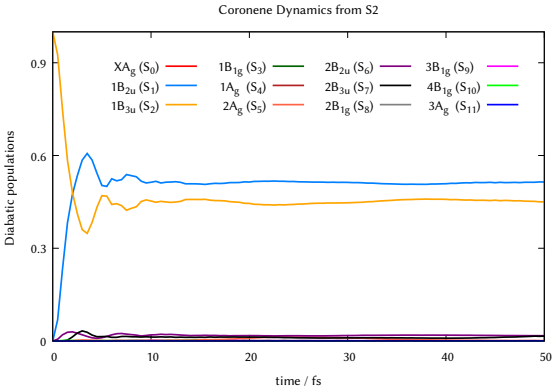

FIG. 8. Diabatic population transfer from $1B_{3u}(S_2)$ electronic excited state of coronene.

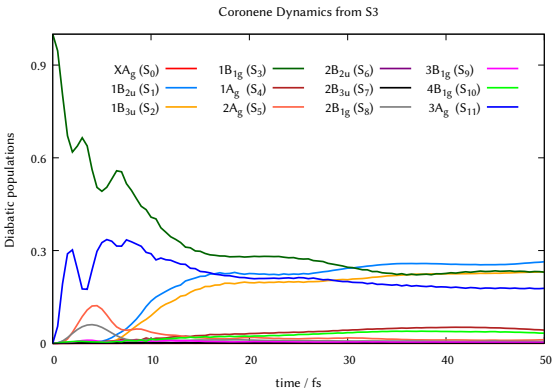

FIG. 9. Diabatic population transfer from $1B_{1g}(S_3)$ electronic excited state of coronene.

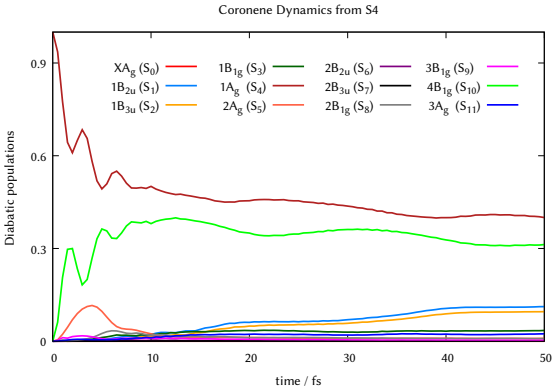

FIG. 10. Diabatic population transfer from $1A_g(S_4)$ electronic excited state of coronene.

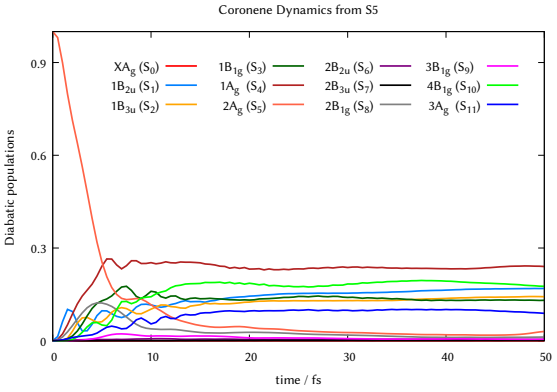

FIG. 11. Diabatic population transfer from $2A_g(S_5)$ electronic excited state of coronene.

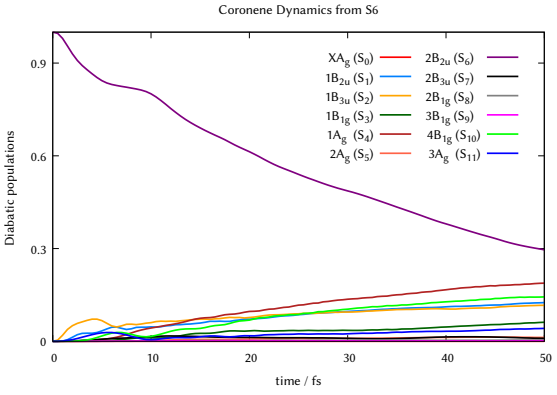

FIG. 12. Diabatic population transfer from $2B_{2u}(S_6)$ electronic excited state of coronene.

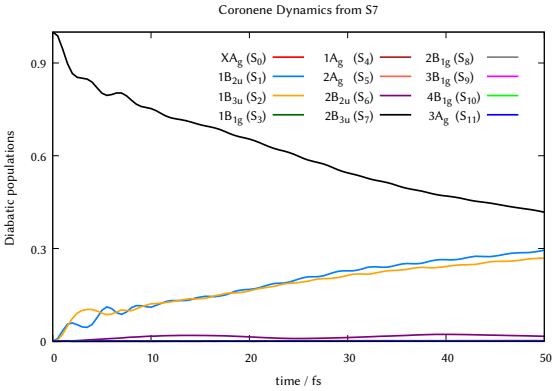

FIG. 13. Diabatic population transfer from $2B_{3u}(S_7)$ electronic excited state of coronene.

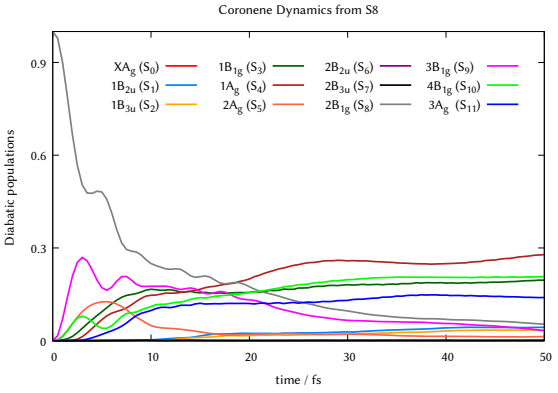

FIG. 14. Diabatic population transfer from $2B_{1g}(S_8)$ electronic excited state of coronene.

IV. EXCITED STATES QUANTUM DYNAMICS OF CIRCUMCORONENE

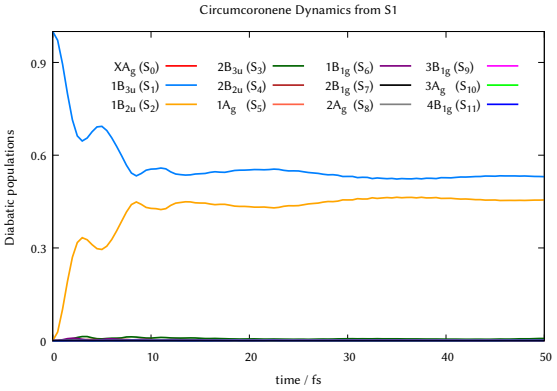

FIG. 15. Diabatic population transfer from $1B_{3u}(S_1)$ electronic excited state of circumnene.

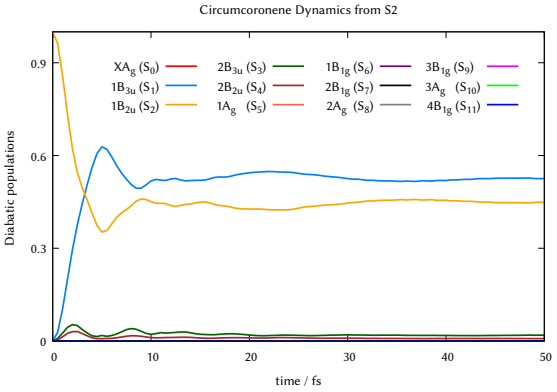

FIG. 16. Diabatic population transfer from $1B_{2u}(S_2)$ electronic excited state of circumnene.

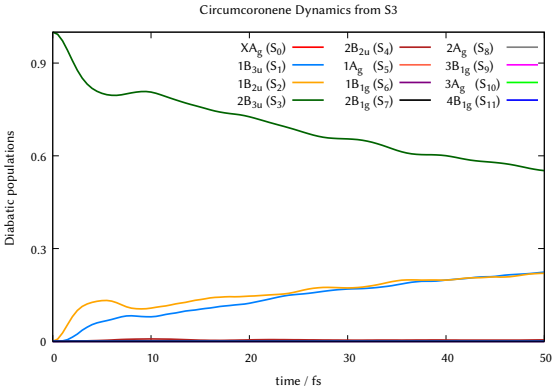

FIG. 17. Diabatic population transfer from $1B_{3u}(S_3)$ electronic excited state of circumnene.

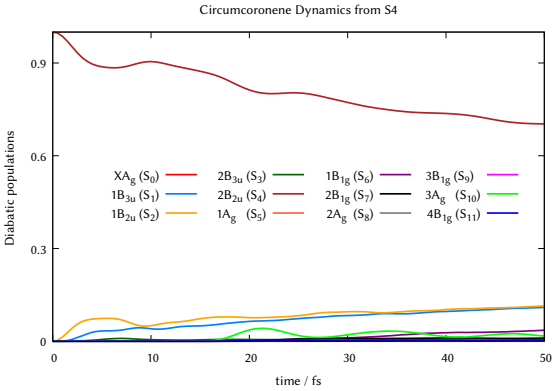

FIG. 18. Diabatic population transfer from $1B_{2u}(S_4)$ electronic excited state of circumnene.

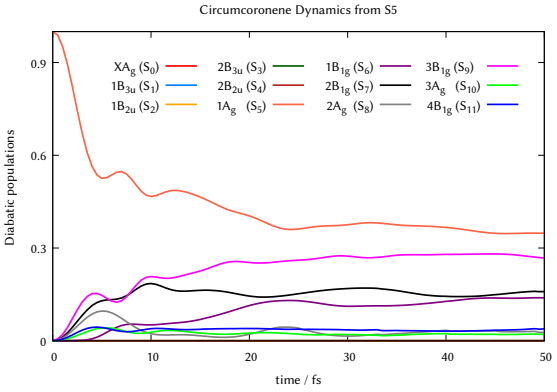

FIG. 19. Diabatic population transfer from $1A_g(S_5)$ electronic excited state of circumnene.

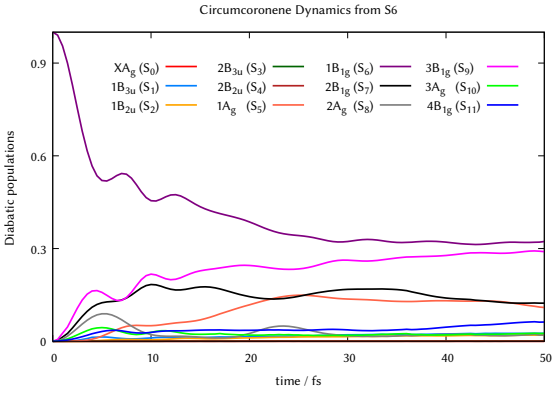

FIG. 20. Diabatic population transfer from $1B_{1g}(S_6)$ electronic excited state of circumnene.

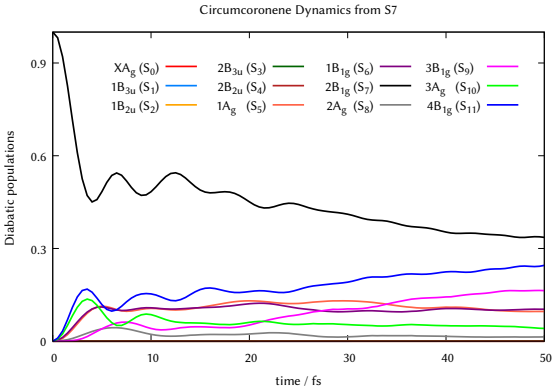

FIG. 21. Diabatic population transfer from $2B_{1g}(S_7)$ electronic excited state of circumnene.

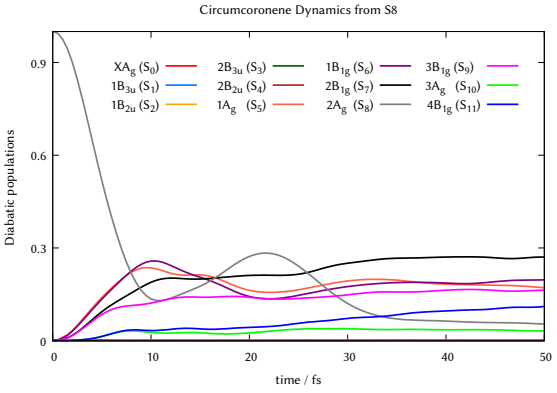

FIG. 22. Diabatic population transfer from $2A_g(S_8)$ electronic excited state of circumnene.

[1] B. Shi, D. Nachtigallová, A. J. Aquino, F. B. Machado, and H. Lischka, J. Chem. Phys. **150** (2019).
[2] S. Hirayama, H. Sakai, Y. Araki, M. Tanaka, M. Imakawa, T. Wada, T. Takenobu, and T. Hasobe, Chem.-Eur. J. **20**, 9081 (2014).